Published in final edited form as:
J Orthop Res. 2014 February ; 32(2): 245–252. doi:10.1002/jor.22516.

Influence of Biochemical Composition on Endplate Cartilage Tensile Properties in the Human Lumbar Spine

Aaron J. Fields, **David Rodriguez**, **Kaitlyn N. Gary**, **Ellen C. Liebenberg**, and **Jeffrey C. Lotz**
Orthopaedic Bioengineering Laboratory, Department of Orthopaedic Surgery, University of California, 513 Parnassus Avenue, S-1157, San Francisco, California 94143-0514

Abstract

Endplate cartilage integrity is critical to spine health and is presumably impaired by deterioration in biochemical composition. Yet, quantitative relationships between endplate biochemical composition and biomechanical properties are unavailable. Using endplate cartilage harvested from human lumbar spines (six donors, ages 51–67 years) we showed that endplate biochemical composition has a significant influence on its equilibrium tensile properties and that the presence of endplate damage associates with a diminished composition–function relationship. We found that the equilibrium tensile modulus (5.9±5.7 MPa) correlated significantly with collagen content (559±147 μg/mg dry weight, r^2=0.35) and with the collagen/GAG ratio (6.0±2.1, r^2=0.58). Accounting for the damage status of the adjacent cartilage improved the latter correlation (r^2=0.77) and indicated that samples with adjacent damage such as fissures and avulsions had a diminished modulus–collagen/GAG relationship (p=0.02). Quasi-linear viscoelastic relaxation properties (C, t_1, and t_2) did not correlate with biochemical composition. We conclude that reduced matrix quantity decreases the equilibrium tensile modulus of human endplate cartilage and that characteristics of biochemical composition that are independent of matrix quantity, that is, characteristics related to matrix quality, may also be important.

Keywords

cartilage endplate; spine; low back pain; intervertebral disc degeneration; biomechanical properties

The structural integrity of the cartilaginous endplate is critical to intervertebral disc health. Proper endplate integrity is important for resisting certain disc herniations[1–4] and tears,[5] maintaining a uniform intradiscal stress distribution,[6] and regulating the transport of disc nutrients and metabolites.[7–9] Importantly, failure of the endplate to perform these functions is hypothesized to accelerate disc degeneration.[6,9] Endplate integrity is also critical for vertebral bone health; endplate cartilage damage significantly associates with inner-vated bone marrow lesions,[10–13] which are suspected to be the pain generator in 30–40% of patients with chronic low back pain (LBP).[14,15] Consequently, elucidating the factors that

Correspondence to: Jeffrey C. Lotz (T: þ1-415-476-7881; F: þ1-415-476-1128; lotzj@orthosurg.ucsf.edu).
The other authors have no conflicts of interest.

influence endplate cartilage integrity is fundamental to understanding the cause of disc degeneration and chronic LBP and could help establish new targets for diagnosis and treatment.

Several factors may influence endplate integrity, including loading conditions[5] and disc behavior.[16,17] The biochemical composition of the cartilage matrix is also presumed essential because the composition determines the material properties of the cartilage, which affect its ability to resist load or deformation. Since excessive load or deformation can damage the tissue, any changes in endplate biochemical composition that diminish its material properties could heighten the risk of damage. Although the composition of the endplate cartilage deteriorates dramatically with age,[18,19] quantitative relationships between composition and material properties are unavailable. We sought to determine this relationship, being the first to report elastic and viscoelastic tensile properties of human endplate cartilage and to relate the presence of endplate cartilage damage to variation in composition and properties.

METHODS

Cadaver Materials

Six lumbar spines were obtained from human cadavers (donor ages 51–67 years; two females, four males) and sectioned into slabs for biomechanical testing and histology. First, the musculature and posterior elements were removed. Next, the spines were cut into four 5- to 7-mm-thick para-sagittal slabs. The slabs were then cut transversely to produce individual bone-disc-bone units. One of the two medial slabs was randomly chosen from each unit and processed for testing; the remaining medial slab was processed for histology (Fig. 1).

Endplate Cartilage Sample Preparation

Endplate cartilage strips cranial and caudal to the disc were removed from the subchondral bone and planed to uniform thickness with a cryostat microtome. Next, dogbone-shaped tensile samples with a 5 mm × 1.5 mm gauge section were punched from the cartilage using a custom die (Fig. 2A), maintaining the gauge section parallel to the AP direction (the primary orientation of the collagen fibrils in the endplate[20]). Final sample thickness was measured with a micrometer designed to sense the tissue's electrical conductivity.[21] All samples were screened with radiography to exclude those with bone fragments in the gauge section (Fig. 2B). Of 25 intact samples, 4 were damaged with the microtome, and 1 was excluded with bone fragments, leaving 20 (Table 1). Samples could not be harvested from 35 levels owing to fluctuations in endplate topology and thickness that precluded the extraction of sufficiently sized samples for testing.

To calculate tissue strains, the central surface of the gauge section was marked with two small steel pins (head diam. 0.75 mm, shaft diam. 0.30 mm) inserted through the thickness (Fig. 2C). This method has the disadvantage of introducing a foreign object, but the fibrous nature of the tissue and its self-sealing properties limit the influence of the pins on tissue behavior. A previous study found that repeated pin insertions were insignificant when compared to other randomizing effects.[22]

Biomechanical Testing

The samples were tested in uniaxial tension using a custom testing apparatus[22,23] consisting of grips to clamp the sample, a stepper motor (ES23B; Parker Hannifin Corp., Rohnert Park, CA) to apply deformation, a precision load cell (SMT1; Interface, Inc., Scottsdale, AZ) to measure force, and a computerized imaging system to calculate strains. The imaging system utilized LabVIEW software (National Instruments, Austin, TX) to capture images, threshold the images to locate the reference points, calculate the strain in the direction of applied deformation, control the motion of the stepper motor, and calculate the stress (force/original cross-sectional area).

At the start of testing, samples were equilibrated in PBS with protease inhibitors (Complete Protease Inhibitor; Roche Applied Science, Indianapolis, IN). After 1 h of equilibration, samples were loaded in the apparatus and preconditioned to establish a repeatable reference configuration. Each sample was stretched to 2% strain over 8 s and held for 10 min before unloading and re-equilibrating at zero force for 10 min. We repeated this preconditioning sequence twice; after the 2nd sequence, the equilibrated state was taken as the reference configuration for the subsequent stress relaxation tests.

Incremental stress relaxation tests[24,25] were performed by applying 2% strain over 8 s. The resulting force was recorded every second during a 10-min relaxation period. Strain increments were repeated until 10% strain (Fig. 3A).

Data Analysis

To calculate the equilibrium elastic properties, the equilibrium tensile stress sσ^e achieved at each strain increment e was fit to an exponential constitutive model $\sigma^e(\varepsilon) = A(e^{B\varepsilon} - 1)$ [24,25] (fig. 3B), where A and B represent material constants. The equilibrium tensile modulus was calculated for the initial part of the stress-strain curve as: $E=\partial\sigma^e/\partial\varepsilon=ABe^{B\varepsilon}$;$E_{\varepsilon=0}=AB$.

To calculate the relaxation properties, the stress-time data from the first relaxation increment was fit to a quasi-linear viscoelastic (QLV) constitutive model[26] (Fig. 3C). The QLV model assumes that the time-dependent relaxation behavior $\sigma(t)$ can be expressed as

$$\sigma(t) = G(t) \times \sigma^c(\varepsilon) \quad (1)$$

In the model, $\sigma^c(\varepsilon)$ is the maximum stress in response to a step input of strain ε, and $G(t)$ is the reduced relaxation function, which represents the time-dependent stress response normalized by the stress at the time of the step in strain. We chose the reduced relaxation function[27]:

$$G(t) = \frac{1 + C\left[E_1(t/\tau_2) - E_1(t/\tau_1)\right]}{1 + C\,ln\,(\tau_2/\tau_1)} \quad (2)$$

where $E_1(y)$ is the exponential integral, and C, t_1, and t_2 are material constants. C is related to energy dissipation in the tissue and t_1, and t_2 are the short and long relaxation constants. To describe the maximum stress response, we chose an exponential model: $\sigma^c(\varepsilon)=A(e^{Be}-$

1).[26] Substituting $\sigma^e(\varepsilon)$ and $G(t)$ into the QLVð model in Equation (1) and integrating over the ramp time yielded an expression for stress relaxation[26]:

$$\sigma\left(t{:}t \geq t_0\right) = \frac{AB\gamma}{1+C\,ln\left(\tau_2/\tau_1\right)} \int_0^{t_0} \left\{1+C\left(E_1\left[\frac{(t-\tau)}{\tau_2}\right] - E_1\left[\frac{(t-\tau)}{\tau_1}\right]\right)\right\} e^{B\gamma\tau}\partial\tau \quad (3)$$

where t_0 is the beginning of the relaxation period following a loading ramp with strain rate γ. To determine the material constants for a set of stress relaxation data, the sum of the squared differences between the experimentally measured stress-time data and the QLV model in Equation (3) was minimized using nonlinear optimization. The optimization scheme was a hybrid approach that consisted of a custom genetic algorithm to identify regions of local minima followed by a Levenberg–Marquardt algorithm to determine the global minimum. The optimization was implemented using MATLAB software (MathWorks, Natick, MA).

Biochemistry

Tissue adjacent to the gauge section was assayed for its water, glycosaminoglycan (GAG), and hydroxyproline contents. First, the tissue was lyophilized to obtain the dry weight. Next, the tissue was digested in papain solution, and GAG content was calculated using the dimethylmethylene blue binding assay.[28] Aliquots were also hydrolyzed in HCl, and hydroxyproline content was calculated.[29] Hydroxyproline content was assumed to be 14% of the total collagen content per dry weight.[30]

Histology

The matching mid-sagittal slabs for each motion segment were processed for histology as described previously.[11] Briefly, slabs were fixed in formalin, radiographed, and decalcified in a mild ion-exchange decalcifying agent (IED; Biocare Medical, Concord, CA). The slabs were then dehydrated in ethanol baths of ascending concentration, cleared in Clearite, and infiltrated with paraffin. Finally, 7-μm-thick sections were microtomed from the paraffin blocks, mounted on slides, and stained with Heidenhain connective tissue stain that contains aniline blue, orange G, and acid fuchsin. Sections were assessed for the presence of endplate damage, with damage classified as[31]: endplate cartilage erosions and avulsions with exposed subchondral bone at the junction of the inner annulus and nucleus pulposus; fissuring of the endplate cartilage; and focal, node-like indentations of the endplate with subchondral bone disruption. Damage was distinguished from sectioning artifacts by noting the cellularity of the adjacent bone marrow and the structure of the adjacent subchondral bone.

Statistical Analysis

The independent role of biochemical composition in the mechanical outcomes was quantified with the Pearson correlation coefficient. We also compared the composition–function relationships between samples with and without histologic evidence of damage using a regression model with three explanatory variables: endplate composition, a categorical variable indicating damage status (corresponds to a change in intercept), and the cross-product between composition and damage status (corresponds to a change in slope). The lower *p*-value among those for slope and intercept differences is reported. Additionally,

mean values of the biochemical and mechanical outcomes were compared between samples with and without damage using unpaired *t*-tests. Statistical analyses were performed using JMP (SAS Institute, Cary, NC). All data are given as mean±SD, unless otherwise noted.

RESULTS

All samples exhibited a nonlinear equilibrium stress–strain relationship that was well described by the 2-parameter exponential model (goodness-offit: 0.98± 0.03). The equilibrium tensile modulus (5.9±5.7 MPa) varied substantially across samples, ranging from <1 to >20 MPa (Table 2). The visco-elastic behavior was characterized by a stress relaxation response with an immediate, rapid drop in stress (t_1=5.7E−5±7.8E−5 s) followed by gradual equilibration after ~6 min (t_2=362±204 s). Collagen content (559±147 μg/mg dry weight) and GAG content (100±32 mg/mg dry weight) were typical of endplate cartilage from 50- to 70-year olds.[18,19]

Collagen content and the ratio of collagen/GAG content correlated best with biomechanical properties (Table 3). The collagen/GAG ratio showed the highest association with the equilibrium tensile modulus (r^2=0.58) and with A (r^2=0.31), whereas collagen content alone showed the highest association with the modulus (r^2=0.35) and with B (r^2=0.24). Neither water nor GAG content was independently associated with any of the biomechanical properties.

The influence of biochemical composition on bio-mechanical properties was significantly different for samples with damage adjacent to the endplate (n=8 endplates) compared to samples without damage (p=0.02). For samples with adjacent damage, the linear relationship between the equilibrium tensile modulus and collagen/GAG ratio had a smaller slope and greater intercept; thus, the stiffest samples with adjacent damage had lower moduli than would be predicted from their collagen/GAG ratios (Fig. 4). Equilibrium properties were lower for samples with damage, consistent with their lower water, GAG, and collagen contents, although differences in individual outcomes were not significant (Table 4).

Endplates with adjacent damage showed cartilage avulsions and fissuring at the junction between the inner annulus and the nucleus pulposus (Fig. 5). In all but one case, the fibrovascular or fatty bone marrow lesions co-located with the endplate damage.

DISCUSSION

The biochemical composition of the endplate had a significant influence on its equilibrium tensile properties. About 58% of the overall variation in equilibrium tensile modulus was explained by the collagen/GAG ratio. Moreover, accounting for endplate damage improved this correlation to explain 77% of the modulus variation, and indicated that samples with adjacent damage had a lower modulus than predicted by their collagen/GAG ratio. Despite the relevance of endplate damage to disc degeneration[6,9] and chronic LBP,[10,12,13] the pathogenesis of endplate damage is not well understood. Any reductions in cartilage material properties are relevant because they could limit the ability of the matrix to resist load or deformation and therefore increase the risk of damage. Our results are important because they establish that reduced tensile modulus correlates with lower collagen content

and collagen/GAG ratios. Collagen content decreases dramatically with age,[18,19] so future work should be aimed at understanding how diminished composition and biomechanical properties factor into the etiology of endplate damage and chronic LBP.

The equilibrium tensile modulus correlated better with the collagen/GAG ratio than with collagen content alone. Although the precise reasons for this are unknown, tensile modulus likely depends not only on the amount of collagen fibrils present to resist deformation, but also on contributions from electrostatic interactions between the positive charges on the collagen and negative charges on the GAGs.[21,32] A second explanation is that GAGs immobilized within the collagen network enhance matrix stiffness.[33]

The finding that samples with adjacent damage had a diminished modulus–collagen/GAG relationship (Fig. 4) suggests that matrix quality may be an important aspect of endplate composition that influences its biomechanical behavior. The collagen/GAG ratio characterizes matrix quantity since it directly relates to the quantities of the individual matrix constituents. Conversely, matrix quality represents characteristics of endplate composition that affect biomechanical behavior but that are not accounted for by matrix quantity, for example, collagen fibril organization and cross-linking. Therefore, any appreciable modification to matrix quality should change the cartilage modulus relative to its collagen/proteoglycan ratio. Although these concepts are frequently applied to bone fragility,[34] and modulus–collagen/GAG relationships were explored in femoral articular cartilage,[21] we are unaware of reports applying the concept of matrix quality to endplate biomechanical behavior. Clearly, additional research is required to elucidate endplate matrix quality, but our findings indicate that such research may clarify the alterations in biomechanical behavior that associate with endplate damage.

The relaxation properties (C, t_1, and t_2) did not correlate with the measured biochemical constituents. Tensile loading might minimize any viscoelastic effects, as a previous study of bovine articular cartilage found that energy dissipation was less significant in tension than in compression.[35] However, Setton et al.[36] determined the viscoelastic compressive properties of endplate cartilage from young baboons and also observed no correlations between material and compositional parameters. An alternative explanation for the lack of a significant relationship is the relatively low water content of the endplate cartilage (~40%). Water content is much higher in articular cartilage(~80%), wherein viscoelastic effects play a greate role.[37] Additional research is necessary to determine which other biochemical constituents are responsible for endplate viscoelastic behavior.

To promote disc health, the biochemical composition of the endplate must meet biomechanical and nutritional demands. Biomechanically, the large degree of structural integration between the cartilaginous and bony endplates[38] and between the cartilaginous end-plate and annulus fibrosus[15,19] suggests that the cartilage must be stiff in tension to resist the tensile loads that develop when the spine is compressed.[5,16,17,39] However, nutritionally the cartilage matrix must contain sufficient pore space to allow nutrient and metabolite transport to and from the avascular disc.[9] The amount of pore space depends on osmotic swelling pressure, and hence, on the relative concentration of GAG and collagen. Roberts et al.[40] measured the transport properties of endplate cartilage from humans aged 5

to 67 years and found that even the endplates with the lowest GAG and collagen concentrations could permit solute transport; in fact, solute transport increased as GAG and collagen concentration decreased because more pore space was available to the solutes. Our results suggest that the equilibrium tensile modulus would decrease because less solid matrix is available to carry load. Together, these findings suggest that endplate tensile properties are inversely related to transport properties. One might speculate that an optimal range of biochemical compositions exists to balance the endplate's bio-mechanical and nutritional demands; identifying this range could clarify the etiology of disc degeneration and have implications for disc regeneration.

Prior work analyzing the histopathology of chronic LBP cases reported that innervated bone marrow lesions bordered endplate cartilage damage[10,12,13] and that damage was not well visualized with conventional MR sequences owing to the tissue's short T2 values.[11,41] Recent studies indicated that new sequences, for example, ultrashort echo time and fast low-angle shot can enhance visualization of the endplate's anatomic details.[42–44] If these sequences can also demonstrate sensitivity to variation in collagen content, then our findings suggest that such sequences could enable noninvasive assessment of endplate biomechanical properties, which might prove useful for prognostic purposes.

We focused on tensile loading since spinal compression appears to induce high tensile stresses in the endplates.[5,16,17,39] The resistance to tensile deformation in cartilage is generated principally by the intrinsic stiffness of the collagen fibrils and entangled GAGs.[45] The equilibrium tensile modulus is a measure of this intrinsic resistance. Another measure relevant to understanding the pathogenesis of endplate damage is tensile strength. Our observation that cartilage fissures and avulsions often occurred near the inner annulus junction is consistent with the anatomy of failure in certain disc herniations[1–3] and tears,[5] and suggests that the tensile strength at the inner annulus junction could also be important. Likewise, compressive loading is physiologically relevant to the end-plates, and thus, the biphasic compressive properties may have additional clinical importance.[36]

We are the first to our knowledge to measure the biomechanical properties of human endplate cartilage, so additional studies are required to confirm these results and extend them to younger individuals with greater collagen and GAG concentrations. For the samples without adjacent damage, the average tensile modulus (6.6±6.9 MPa) is similar to that reported for femoral articular cartilage in adults (6.0±4.5 MPa),[21] and comparison of the composition–function relationships between endplate and femoral cartilage indicated a similar effect of the collagen/GAG ratio on tensile modulus (p=0.19 for differences in slope). Thus, despite the absence of endplate cartilage biomechanical studies for comparison, the consistency of our findings with those from femoral cartilage supports their validity.

This study had several limitations. All samples were obtained from mid-sagittal sections and were tested in the AP direction. We did not evaluate intraendplate heterogeneity or anisotropy. The cross-sectional study design prevented us from concluding whether endplate damage was a cause or effect of the diminished composition–function relationship. For example, other factors such as differences in loading[5] or the mechanical properties of the

osteochondral interface[38] could influence endplate cartilage stress and therefore contribute independently to damage risk. Finally, the small sample size was derived from adults with a narrow age range; expansion to larger and younger cohorts is required to confirm some of the findings. In particular, none of the relaxation properties correlated significantly with biochemical composition. A larger sample size with younger individuals may have greater variations in composition and properties, which could increase its role.

In conclusion, we provide quantitative data regarding the influence of biochemical composition on material properties in human endplate cartilage. Using biomechanical testing, biochemical analysis, and histology, we found that endplate collagen content and collagen/GAG ratios significantly influence equilibrium tensile properties and that the presence of endplate damage associates with a diminished composition– function relationship. These quantitative relationships help bridge a knowledge gap between deterioration in endplate composition[18,19] and loss in endplate bio-mechanical function. This motivates future work to understand how diminished endplate composition and function factors into the etiology of endplate damage and chronic LBP.

Acknowledgments

The authors thank Alberto Lovell, Rachel Willardson, Elaine Soohoo, and Suraj Bhogal for their technical assistance. Dr. Lotz is a consultant for Relievant Medsystems, who provided partial support for this study.

Grant sponsor: NIH; Grant number: AR052811.

REFERENCES

1. Harada Y, Nakahara S. A pathologic study of lumbar disc herniation in the elderly. Spine. 1989; 14:1020–1024. [PubMed: 2476860]
2. Rajasekaran S, Bajaj N, Tubaki V, et al. ISSLS prize winner: the anatomy of failure in lumbar disc herniation: an in vivo, multimodal, prospective study of 181 subjects. Spine. 2013; 38:1491–1500. [PubMed: 23680832]
3. Tanaka M, Nakahara S, Inoue H. A pathologic study of discs in the elderly. Separation between the cartilaginous endplate and the vertebral body. Spine. 1993; 18:1456–1462. [PubMed: 8235816]
4. Vernon-Roberts B, Moore RJ, Fraser RD. The natural history of age-related disc degeneration: the pathology and sequelae of tears. Spine. 2007; 32:2797–2804. [PubMed: 18246000]
5. Veres SP, Robertson PA, Broom ND. ISSLS prize winner: how loading rate influences disc failure mechanics: a microstructural assessment of internal disruption. Spine. 2010; 35:1897–1908. [PubMed: 20838275]
6. Adams MA, Freeman BJ, Morrison HP, et al. Mechanical initiation of intervertebral disc degeneration. Spine. 2000; 25:1625–1636. [PubMed: 10870137]
7. Rodriguez AG, Slichter CK, Acosta FL, et al. Human disc nucleus properties and vertebral endplate permeability. Spine. 2011; 36:512–520. [PubMed: 21240044]
8. Rajasekaran S, Babu JN, Arun R, et al. ISSLS prize winner: a study of diffusion in human lumbar discs: a serial magnetic resonance imaging study documenting the influence of the endplate on diffusion in normal and degenerate discs. Spine. 2004; 29:2654–2667. [PubMed: 15564914]
9. Urban JP, Smith S, Fairbank JC. Nutrition of the intervertebral disc. Spine. 2004; 29:2700–2709. [PubMed: 15564919]
10. Brown MF, Hukkanen MV, McCarthy ID, et al. Sensory and sympathetic innervation of the vertebral end-plate in patients with degenerative disc disease. J Bone Joint Surg Br. 1997; 79:147–153. [PubMed: 9020464]

11. Fields AJ, Liebenberg EC, Lotz JC. Innervation of pathologies in the lumbar vertebral endplate and intervertebral disc. Spine J. Oct 18.2013
12. Modic MT, Steinberg PM, Ross JS, et al. Degenerative disk disease: assessment of changes in vertebral body marrow with MR imaging. Radiology. 1988; 166:193–199. [PubMed: 3336678]
13. Ohtori S, Inoue G, Ito T, et al. Tumor necrosis factor-immunoreactive cells and PGP 9.5-immunoreactive nerve fibers in vertebral endplates of patients with discogenic low back pain and modic Type 1 or Type 2 changes on MRI. Spine. 2006; 31:1026–1031. [PubMed: 16641780]
14. Albert HB, Briggs AM, Kent P, et al. The prevalence of MRI-defined spinal pathoanatomies and their association with modic changes in individuals seeking care for low back pain. Eur Spine J. 2011; 20:1355–1362. [PubMed: 21544595]
15. Lotz JC, Fields AJ, Liebenberg EC. The role of the vertebral endplate in low back pain. Global Spine J. 2013; 3:153–164. [PubMed: 24436866]
16. Fields AJ, Lee GL, Keaveny TM. Mechanisms of initial endplate failure in the human vertebral body. J Biomech. 2010; 43:3126–3131. [PubMed: 20817162]
17. Kurowski P, Kubo A. The relationship of degeneration of the intervertebral disc to mechanical loading conditions on lumbar vertebrae. Spine. 1986; 11:726–731. [PubMed: 3787344]
18. Antoniou J, Goudsouzian NM, Heathfield TF, et al. The human lumbar endplate. Evidence of changes in biosynthesis and denaturation of the extracellular matrix with growth, maturation, aging, and degeneration. Spine. 1996; 21:1153–1161. [PubMed: 8727189]
19. Roberts S, Menage J, Urban JP. Biochemical and structural properties of the cartilage end-plate and its relation to the intervertebral disc. Spine. 1989; 14:166–174. [PubMed: 2922637]
20. Aspden RM, Hickey DS, Hukins DW. Determination of collagen fibril orientation in the cartilage of vertebral end plate. Connect Tissue Res. 1981; 9:83–87. [PubMed: 6458450]
21. Akizuki S, Mow VC, Müller F, et al. Tensile properties of human knee joint cartilage: I. Influence of ionic conditions, weight bearing, and fibrillation on the tensile modulus. J Orthop Res. 1986; 4:379–392. [PubMed: 3783297]
22. Wagner DR, Lotz JC. Theoretical model and experimental results for the nonlinear elastic behavior of human annulus fibrosus. J Orthop Res. 2004; 22:901–909. [PubMed: 15183453]
23. Bass EC, Ashford FA, Segal MR, et al. Biaxial testing of human annulus fibrosus and its implications for a constitutive formulation. Ann Biomed Eng. 2004; 32:1231–1242. [PubMed: 15493511]
24. Huang CY, Stankiewicz A, Ateshian GA, et al. Anisotropy, inhomogeneity, and tension-compression nonlinearity of human glenohumeral cartilage in finite deformation. J Biomech. 2005; 38:799–809. [PubMed: 15713301]
25. Elliott DM, Guilak F, Vail TP, et al. Tensile properties of articular cartilage are altered by meniscectomy in a canine model of osteoarthritis. J Orthop Res. 1999; 17:503–508. [PubMed: 10459755]
26. Abramowitch SD, Woo SL. An improved method to analyze the stress relaxation of ligaments following a finite ramp time based on the quasi-linear viscoelastic theory. J Biomech Eng. 2004; 126:92–97. [PubMed: 15171134]
27. Fung YC. Elasticity of soft tissues in simple elongation. Am J Physiol. 1967; 213:1532–1544. [PubMed: 6075755]
28. Farndale RW, Buttle DJ, Barrett AJ. Improved quantitation and discrimination of sulphated glycosaminoglycans by use of dimethylmethylene blue. Biochim Biophys Acta. 1986; 883:173–177. [PubMed: 3091074]
29. Woessner JF Jr. The determination of hydroxyproline in tissue and protein samples containing small proportions of this imino acid. Arch Biochem Biophys. 1961; 93:440–447. [PubMed: 13786180]
30. Neuman RE, Logan MA. The determination of hydroxyproline. J Biol Chem. 1950; 184:299–306. [PubMed: 15421999]
31. Boos N, Weissbach S, Rohrbach H, et al. Classification of age-related changes in lumbar intervertebral discs: 2002 Volvo Award in basic science. Spine. 2002; 27:2631–2644. [PubMed: 12461389]

32. Mathews MB. The interaction of collagen and acid mucopolysaccharides. A model for connective tissue. Biochem J. 1965; 96:710–716. [PubMed: 4222034]
33. Muir H. Proteoglycans as organizers of the intercellular matrix. Biochem Soc Trans. 1983; 11:613–622. [PubMed: 6667766]
34. Hernandez CJ, Keaveny TM. A biomechanical perspective on bone quality. Bone. 2006; 39:1173–1181. [PubMed: 16876493]
35. Park S, Ateshian GA. Dynamic response of immature bovine articular cartilage in tension and compression, and nonlinear viscoelastic modeling of the tensile response. J Biomech Eng. 2006; 128:623–630. [PubMed: 16813454]
36. Setton LA, Zhu W, Weidenbaum M, et al. Compressive properties of the cartilaginous end-plate of the baboon lumbar spine. J Orthop Res. 1993; 11:228–239. [PubMed: 8483035]
37. Mow VC, Kuei SC, Lai WM, et al. Biphasic creep and stress relaxation of articular cartilage in compression: Theory and experiments. J Biomech Eng. 1980; 102:73–84. [PubMed: 7382457]
38. Paietta RC, Burger E, Ferguson VL. Mineralization and collagen orientation throughout aging at the vertebral endplate in the human lumbar spine. J Struct Biol. Aug 30.2013
39. Shirazi-Adl SA, Shrivastava SC, Ahmed AM. Stress analysis of the lumbar disc-body unit in compression: a three-dimensional nonlinear finite element study. Spine. 1984; 9:120–134. [PubMed: 6233710]
40. Roberts S, Urban JP, Evans H, et al. Transport properties of the human cartilage endplate in relation to its composition and calcification. Spine. 1996; 21:415–420. [PubMed: 8658243]
41. Benneker LM, Heini PF, Anderson SE, et al. Correlation of radiographic and MRI parameters to morphological and biochemical assessment of intervertebral disc degeneration. Eur Spine J. 2005; 14:27–35. [PubMed: 15723249]
42. Bae WC, Statum S, Zhang Z, et al. Morphology of the cartilaginous endplates in human intervertebral disks with ultrashort echo time MR imaging. Radiology. 2013; 266:564–574. [PubMed: 23192776]
43. Law T, Anthony MP, Chan Q, et al. Ultrashort time-to-echo MRI of the cartilaginous endplate: technique and association with intervertebral disc degeneration. J Med Imaging Radiat Oncol. 2013; 57:427–434. [PubMed: 23870338]
44. Moon SM, Yoder JH, Wright AC, et al. Evaluation of intervertebral disc cartilaginous endplate structure using magnetic resonance imaging. Eur Spine J. 2013; 22:1820–1828. [PubMed: 23674162]
45. Setton LA, Elliott DM, Mow VC. Altered mechanics of cartilage with osteoarthritis: human osteoarthritis and an experimental model of joint degeneration. Osteoarthritis Cartilage. 1999; 7:2–14. [PubMed: 10367011]

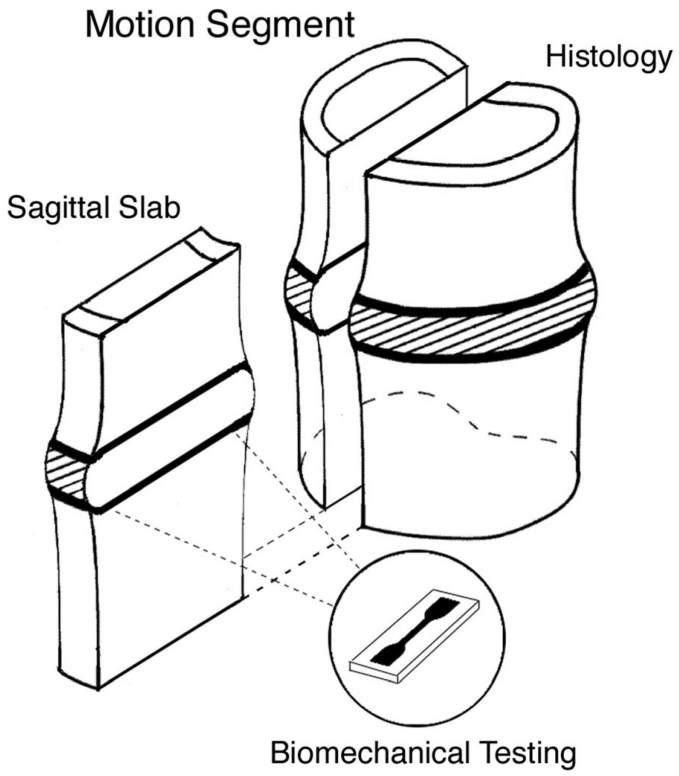

Figure 1.

Bone-disc-bone motion segment with mid-sagittal slab extracted for endplate cartilage dissection and biomechanical testing. A matching mid-sagittal slab from each motion segment was processed for histology to assess for the presence of any endplate damage.

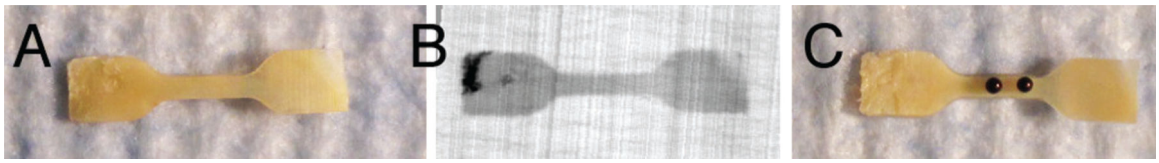

Figure 2.

(A) Cartilage sample punched from the endplate using a dogbone-shaped die. Gauge section dimensions: 5 mm × 1.5 mm. (B) Radiographs were used to screen samples for the presence of calcified cartilage and bone in the gauge section. Note the bits of bone (opaque areas) in the grip section of the sample. (C) Sample with black reference points for strain calculations.

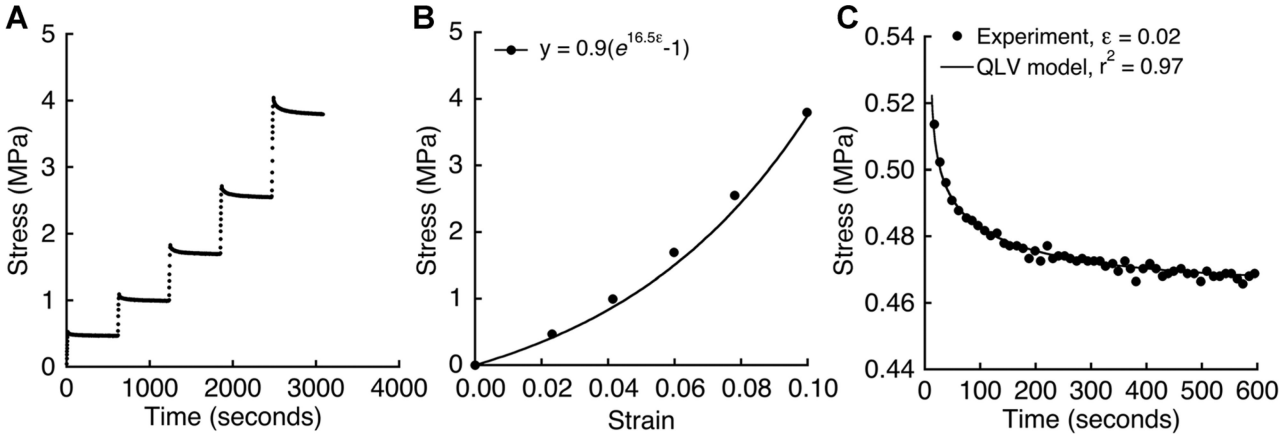

Figure 3.

(A) Example of stress-time behavior in response to 2% strain increments applied after 10-min relaxation periods. (B) Equilibrium stress versus applied strain for the incremental loading in panel A. (C) Stress relaxation behavior after the first strain increment in panel A. Stress-time data were fit to a five-parameter QLV model using nonlinear optimization (see the Methods Section for model details).

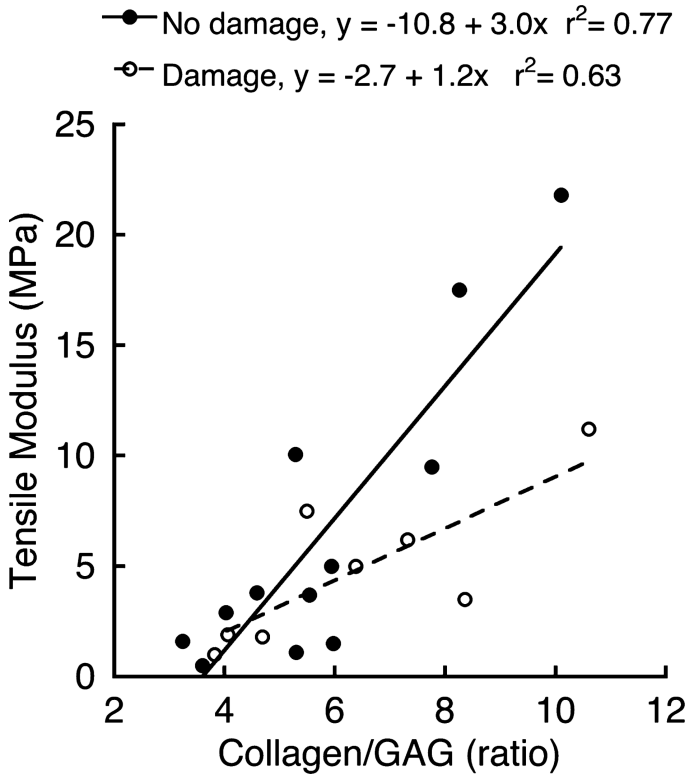

Figure 4.

The relationship between equilibrium tensile modulus and collagen/GAG ratio was significantly different for samples from levels with histologic evidence of endplate damage compared to samples from levels without endplate damage (p=0.02).

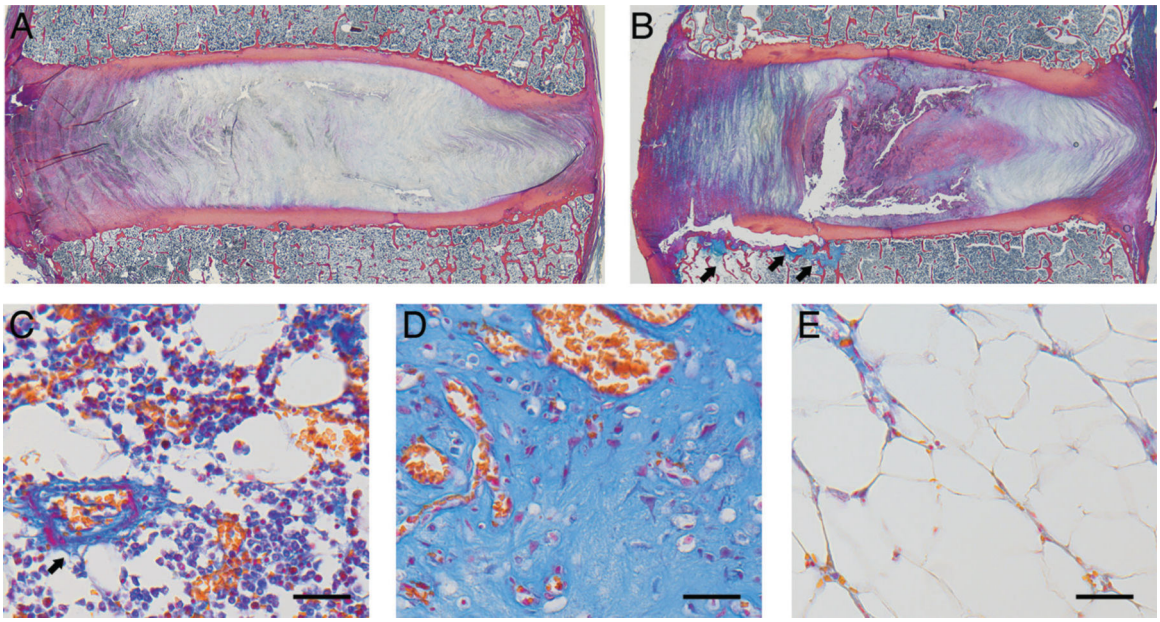

Figure 5.

(A) Mid-sagittal histology section from a spinal level with an intact cartilage endplate. (B) Endplates with damage were typified by cartilage avulsions and fissures at the interface between the inner annulus and nucleus pulposus. Note the fibrovascular and fatty marrow reactions adjacent to the location of the endplate damage (arrows). (C) Normal hematopoietic endplate marrow with blood vessel (arrow) and vascular sinusoids. (D) Richly vascularized endplate marrow with dense fibrous tissue corresponding to the arrows in panel B. (E) Fatty marrow with low cellularity corresponding to the leftmost arrow in panel B. In all panels, left side is anterior. In panels C–E, scale bars are 50 μm. Heidenhain connective tissue stain.

Table 1

Donor Age, Sex, and Spinal Level for $n = 20$ Endplate Cartilage Samples

Donor No.	Age (Years)	Sex	Levels[a]
1	51	Male	L2i, L3s, L4s, L5i, S1s
2	57	Male	L4i, L5s, L5i, S1s
3	60	Male	L3i
4	61	Female	L5s
5	63	Female	L1i, L2s, L3i, L4i, L5i
6	67	Male	L3i, L4s, L5i, S1s

[a]Levels denote cartilage samples taken from the superior (s) and inferior (i) endplate of a given vertebra.

Table 2

Biomechanical and Compositional Data for Samples Included in the Study (n = 20 Endplates)

	Mean	SD	CV (%)	Range
Equilibrium properties				
A (MPa)	0.24	0.25	104.2	0.02–0.92
B	26.8	13.7	51.1	10.9–67.4
Tensile modulus, $E_{0\%}$ (MPa)	5.9	5.7	96.6	0.5–21.8
Viscoelastic properties				
Energy dissipation, C (MPa)	0.035	0.016	45.7	0.015–0.065
Short relaxation constant, τ_1 (s)	5.7E–5	7.8E–5	135.8	8.7E–8–2.7E–4
Long relaxation constant, τ_2 (s)	362	204	56.4	129–766
Biochemical composition				
Water content (%)	39.7	11.0	27.7	22.1–62.4
GAG content (μg/mg dry wt)	99.8	31.7	31.8	43.7–184.8
Collagen content (μg/mg dry wt)	558.5	146.9	26.3	329.0–886.9

Table 3

Independent Role (Pearson's Correlation Coefficient, *r*) of Endplate Biochemical Composition on Biomechanical Properties (*n* = 20 Endplates)

	Collagen/GAG Ratio	Collagen Content	GAG Content	Water Content
A (MPa)	0.56[b]	0.20	–0.38	0.09
B	0.19	0.49[a]	0.02	–0.04
Tensile modulus, $E_{0\%}$	0.76[c]	0.59[b]	–0.34	0.07
Energy dissipation, *C*	–0.34	–0.33	0.17	0.03
Short relaxation constant, τ_1	0.03	–0.02	–0.14	–0.01
Long relaxation constant, τ_2	0.20	0.19	–0.06	0.13

[a] $p < 0.05$.

[b] $p < 0.01$.

[c] $p < 0.001$.

Table 4

Comparison of Mean Biomechanical Properties and Biochemical Composition Between Endplate Cartilage Samples With and Without Histologic Evidence of Damage

	No Damage (n = 12 Endplates)	Damage (n = 8 Endplates)	% Difference[a]	p-Value
A (MPa)	0.25 ± 0.19	0.22 ± 0.12	–15.4	0.74
B	30.5 ± 10.2	21.2 ± 5.8	–30.2	0.15
Tensile modulus, $E_{0\%}$ (MPa)	6.6 ± 4.4	4.8 ± 3.5	–27.7	0.50
Energy dissipation, C (MPa)	0.031 ± 0.010	0.041 ± 0.013	31.3	0.18
Short relaxation constant, τ_1 (s)	4.7E–5 ± 5.3E–5	7.3E–5 ± 6.7E–5	55.3	0.48
Long relaxation constant, τ_2 (s)	382 ± 132	336 ± 187	–12.1	0.64
Water content (%)	42.3 ± 7.3	35.8 ± 8.1	–15.4	0.15
GAG content (μg/mg dry wt)	108.3 ± 21.3	87.1 ± 21.3	–19.6	0.20
Collagen content (μg/mg dry wt)	593.4 ± 107.8	506.1 ± 75.2	–14.7	0.20

Data given as mean ± 95% CI.

[a] Percent difference calculated with respect to the “No damage” mean values.